Versatile Two-Step Functionalization of Nanocarbons: Grafting of Propargylic Groups and Click Post-Functionalization
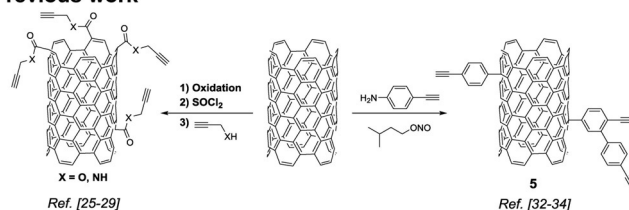
Antonin Desmecht, Sophie Hermans,* and Olivier Riant*[a]

Chemical functionalization of nanocarbons is essential for further applications in various fields. We developed a facile, inexpensive, and gram-scale one-pot route towards alkynyl-functionalized nanocarbons. Nucleophilic addition/propargylic capture places alkyne moieties at the surface of carbon nanotubes (CNTs) and graphene. Thermogravimetric analysis coupled with mass spectrometry and Raman analysis confirmed the efficiency of this process. Conductivity measurements demonstrated the maintenance of the CNT electrical properties. The attached alkynyl moieties were reacted with various azide derivatives through the click-Huisgen [3+2] cycloaddition and characterized with XPS. The efficient addition of those derivatives enables the application of our finding in various fields. This route is a reliable and convenient alternative to the known diazonium functionalization and oxidation-esterification reactions to graft alkyne groups.
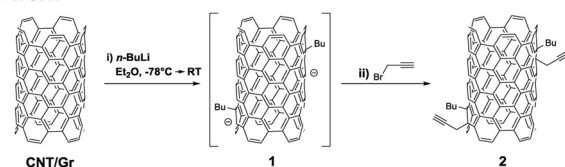
The chemical modification of nanocarbons [such as carbon nanotubes (CNTs) and graphene][1-4] allows their use in various applications such as sensors,[5] biomedical vectors,[6] nanocomposites,[7,8] electronics,[9] energy storage devices,[10] and heterogeneous catalysts.[11] Indeed, in their pristine state, CNTs and graphene sheets tend to stack through π–π stacking. Such bundles affect their solubility in most organic solvents and water. Therefore, the race for new functionalization protocols featuring high loading, reproducibility, robustness, and homogeneity of functions is still on, especially in the case of graphene. We decided to exploit the two-step nucleophilic addition of organolithium compounds and electrophile capture grafting.[12-14] This method has already been used for the trapping of different electrophiles, either alkanes for dispersion

purposes[15,16] or other dead-end moieties.[14,17-21] We, hereby, propose the use of a new, easily accessible, cheap, and atom-efficient electrophile: propargyl bromide (Scheme 1). The nucleophilic addition of nBuLi at the CNT surface generates anionically charged tubes, known as nanotubides. The electrostatic repulsion of such nanotubides promotes their dispersion in solvents. The anionic intermediate subsequently and efficiently traps the electrophile, leading to an alkyne-modified support. Thereafter, the alkynyl functional groups were extensively used for various copper(I)-catalyzed alkyne-azide cycloadditions (CuAACs).[22] This "click-reaction", as described by Sharpless et al.,[23,24] offers a versatile and efficient post-functionalization method. To this day, only two methods are usually employed for the grafting of alkynyl moieties on CNTs/graphene: the amidation or esterification of carboxylic groups (inherent with nanocarbon synthesis or increased with acidic/oxidative treatment)[25-29] and the Tour reaction,[30,31] using ethynylaniline.[32-34] Several drawbacks are known regarding these two reactions. In the first case, an oxidative pre-treatment is required for an efficient loading. This prerequisite can cause a shortening of the CNTs or even cause them to collapse. It induces the partial or complete loss of properties, especially electric conductivity, often crucially needed in composite materials. In the second case, the formation of multiple aryl layers through biaryl coupling has already been outlined.[35]

[a] A. Desmecht, Prof. S. Hermans, Prof. O. Riant
Institute of Condensed Matter and Nanosciences
Molecules, Solids and Reactivity (IMCN/MOST)
Université catholique de Louvain
Place Louis Pasteur 1, 1348 Louvain-la-Neuve (Belgium)
E-mail: sophie.hermans@uclouvain.be
olivier.riant@uclouvain.be

Scheme 1. Chemical functionalization of nanocarbons for the grafting of alkyne functional groups.

We started our investigation with multi-walled nanotubes (MWNTs), as the external layer can be functionalized whilst the internal layers keep the material's integrity. Spectroscopic in-

vestigations were also performed on single-walled nanotubes (SWNTs) as well as on graphene. TEM images of the pristine (*p*)-MWNTs used in this work showed an average of 10 concentric graphene layers per tube (see Figure S1 in the Supporting Information). We chose to work with *n*BuLi instead of other butyl-isomers, because it exhibits less steric hindrance and is safer to use.[15] Good dispersion of nanotubides **1** was observed, in accordance with the reaction mechanism. Thereafter, those charges captured propargylic groups through reaction with propargyl bromide to give material **2**. The grafting efficiency was evaluated by using thermogravimetric analysis coupled with mass spectrometry (TGA-MS). TGA showed a first weight loss in the range 150–600 °C, 4.0 % for functionalized (*f*)-MWNT **2** and 14.6 % for *f*-SWNT **2**, which was attributed to the elimination of the grafted groups (Figure 1). The degree of functionalization can be evaluated as 1 in 97 carbons for *f*-MWNT and 1 in 23 carbons for *f*-SWNT. This significant difference is easily explained by the fact that, in the first case, only the external layer is available for grafting. Taking into account the 10 concentric layers of the MWNTs, the external degree of functionalization can be evaluated as 1 in 13 carbons. A second weight loss was observed in the range of 650–900 °C, owing to the decomposition of the tubes. The MS analysis confirmed the existence of both butyl (m/z 57) and propargylic groups (m/z 39) during the first weight loss. Notably, our methodology is scalable up to 1 g of MWNTs.
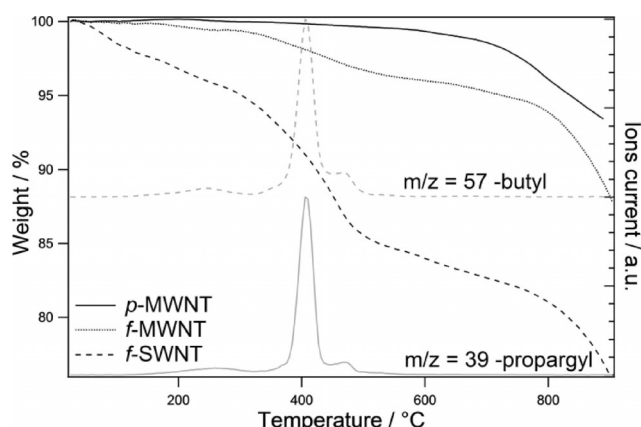

Figure 1. TGA-MS graph recorded under a N_2 atmosphere.

Raman spectroscopy is intensively used to validate the covalent nature of the functionalization. The defect (D) band (ca. 1300 cm^{-1}) and graphitic (G) band (ca. 1590 cm^{-1}) are compared. The ratio of intensity of the D to G bands (I_D/I_G) increases with the attachment of external moieties, as the sp^3 contribution increases. We actually noted an increase in this ratio from 0.13 to 0.29 for SWNTs (Figure 2 a). Exfoliated graphene has a perfectly plane structure and, thus, a very low reactivity. Nonetheless, the appearance of the D band was observed for alkyne-functionalized graphene (*f*-Gr) (Figure 2 b). The 2D band full-width half-maximum of 32 cm^{-1} and its single Lorentzian shape demonstrate the single-sheet character of the material (see Figure S3 in the Supporting Information).[36]
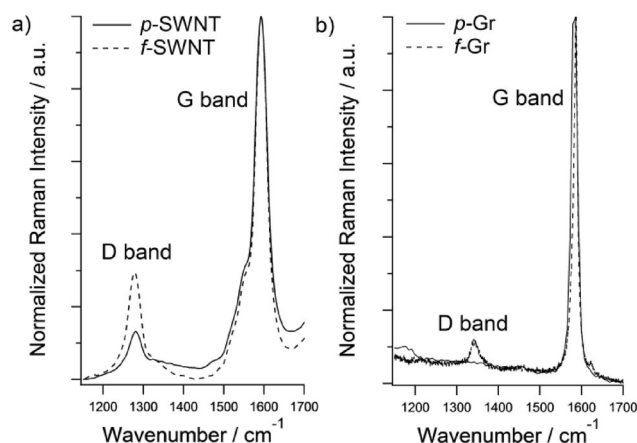

Figure 2. a) Raman spectra ($\lambda = 1064$ nm) of *p*-SWNT (——) and *f*-SWNT (-----), and b) Raman spectra ($\lambda = 514$ nm) of *p*-Gr (——) and *f*-Gr (-----).
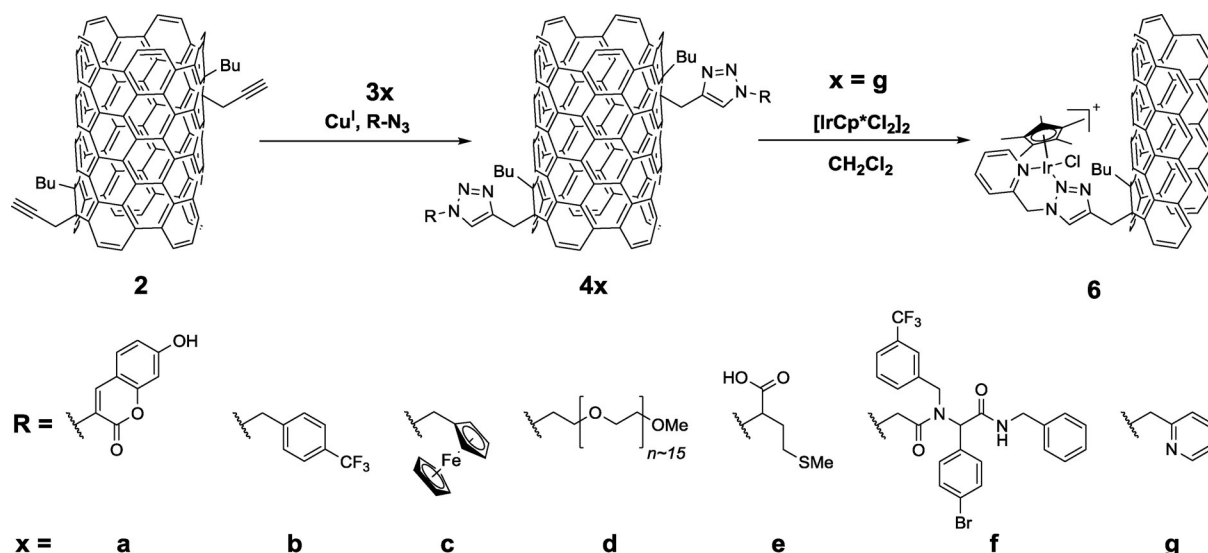
We then investigated the conductivity of **2** with respect to *p*-MWNTs for comparison with the ethynylphenyl-functionalized nanotubes **5** using Tour's reaction. Functionalization of the sidewall of the nanotubes and the resulting sp^2 framework perturbation is known to decrease or annihilate the electrical properties of the material. The conductivity of *p*-MWNTs used in this work was evaluated to be 81 S cm^{-1} (Table 1). This conductivity was only reduced by half when the propargyl moieties were introduced, thanks to our methodology (38 S cm^{-1}). However, when Tour's reaction was employed, a significant drop to 3.1 S cm^{-1} was measured for a similar functionalization degree. This noticeable difference can be put to use in nanocomposite applications, where electrical conduction is highly desirable. Preservation of the nanocarbon properties has been nicely described by Wang and co-workers in the different, yet similar, Billups–Birch reductive functionalization.[37] They proposed a banded functionalization of SWNTs. Intact and functionalized segments are alternated with each other. This enables the conservation of conduction properties in the SWNTs through the sustained band structures of sp^2-hybridized carbons.

Table 1. Electrical properties of *p*-MWNTs and f-MWNTs.

Sample	Conductivity [S cm^{-1}][a]	Loading [wt %]	Functionalization degree
p-MWNTs	81 ± 10	0	–
MWNT-2	38 ± 4	4.0	1:97
MWNT-5	3.1 ± 0.7	12.2	1:60
[a] Measured according to Smits' procedure.[38]			

Moving a step forward, the click-Huisgen reaction was performed on the alkyne-modified tubes (Scheme 2). "Click chemistry" is a very interesting tool for the post-functionalization of *f*-CNTs. It benefits from complete or near-to-complete conversion under mild reaction conditions with almost no side product formation.[23] Yet, the most valuable feature is the

Scheme 2. CuAAC post-functionalization.

(bio-)orthogonality of the reaction. The copper-catalyzed reaction of azido and terminal alkyne reagents generates the 1,4-substituted triazole ring in a regioselective manner. This cyclization was confirmed with the help of 7-hydroxycoumarin, a fluorescent probe. The non-emissive azido-coumarin **3a** becomes fluorescent when its azido group is transformed into triazole (Figure 3a).[39] When **3a** was clicked onto SWNT-**2**, an increased emission at 450 nm was observed (Figure 3b) and, therefore, confirmed the cycloaddition. The efficiency and versatility of the Huisgen reaction was highlighted with different substrates and confirmed by using X-ray photoelectron spectroscopy (XPS) (Table 2) and qualitative tests (Figure 4). The catalytic system used involves copper iodide as the Cu^I source and *N,N,N′,N′′,N′′*-pentamethyldiethylenetriamine (PMDETA) as the stabilizing ligand (see Section 2e, Procedure B in the Supporting Information).
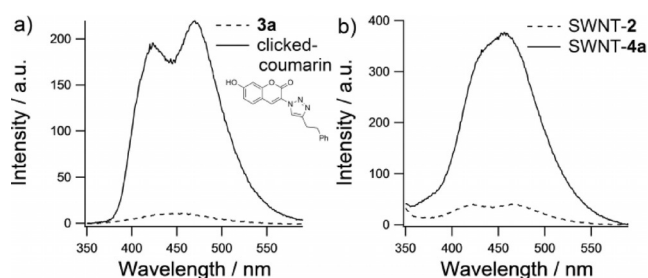
Table 2. Characterization of post-functionalized MWNTs by using XPS [at %].[a]

Entry	C_{1s}	O_{1s}	N_{1s}	F_{1s}	Fe_{2p}	S_{2p}	Br_{3d}	Ir_{4f}
4a	87.88	9.83	2.29	–	–	–	–	–
4b	93.19	4.14	1.27	1.40	–	–	–	–
4c	94.14	3.80	1.80	–	0.26	–	–	–
4d	91.20	7.60	1.23	–	–	–	–	–
4e	94.41	4.12	1.20	–	–	0.27	–	–
4f	93.28	3.71	1.80	1.06	–	–	0.15	–
4g	95.87	2.40	1.73	–	–	–	–	–
6	95.78	2.39	1.49	–	–	–	–	0.27

[a] See Scheme 2 for meaning of entry.

Figure 3. Emission spectra of a) **3a** (----) and clicked coumarin (——) as well as b) SWNT-**2** (----) and SWNT-**4a** (——), suspended in H_2O 9:1 DMSO, 4 wt % SDS ($\lambda_{exc} = 310$ nm).
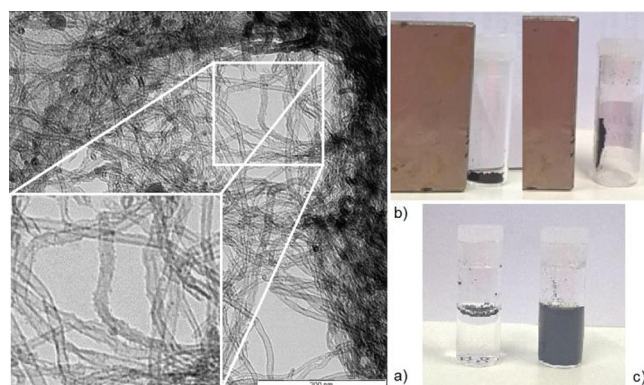

Figure 4. a) TEM image of **4c** after thermal treatment under a N_2 atmosphere, b) magnetic response of **4c** before (left) and after (right) thermal treatment, and c) difference of solvent affinity between **2** (left) and **4d** (right) in water after 2 min sonication.

4-Trifluoromethylbenzyl azide **3b** was first used as a simple fluorine-tagged substrate for quantification of post-functionalization efficiency. XPS analysis revealed the presence of 1.40 at % fluorine and 1.27 at % nitrogen at the surface (Table 2, entry 1). The expected atomic ratio of 1 between F and N (as there are three nitrogen atoms for three fluorine

atoms) is confirmed with an experimental value of 1.1. The cycloaddition of azidomethylferrocene **3c** (Table 2, entry 2) and the subsequent thermal treatment of the resulting material enabled the formation of iron oxide nanoparticles. Magnetic nanoparticles, either as a core material or decorating a solid

support, are regularly used in heterogeneous catalysis, as magnetic decantation is preferred over filtration.[40–42] Such nanoparticles could be seen on the outside of the MWNTs by using transmission electron microscopy (TEM) (Figure 4a). Their magnetic response was also observed (Figure 4b). PEGylated chains could also be anchored at the surface of the tubes with a loading of 26.54 wt% (calculated from 1.23 at% N; Table 2, entry 3). The direct effect of this grafting is the switch from a hydrophobic material to a hydrophilic one (Figure 4c). This change is highly valuable for medicinal applications, where water-soluble CNTs exhibit less cytotoxicity and oxidative stress when compared to their insoluble counterparts.[6,43,44]

Azido-modified methionine **3e** could also be attached at the surface of the MWNTs (0.27 at% S; Table 2, entry 4). Amino acids are known to be interesting building blocks for the synthesis of polypeptides. They can be used, for instance, for cell recognition and tumor targeting.[45] More complex molecules such as the Ugi adduct **3f** are also compatible with our methodology. Although less bromine than expected is measured (0.15 at%; Table 2, entry 5), the experimental nitrogen/fluorine atomic ratio is consistent with the theoretical value (1.70 vs. 1.67). Azidomethylpyridine **3g** was efficiently clicked to yield a bidentate click ligand supported on MWNTs **4g** (1.73 at% N; Table 2, entry 6). Such click ligands are known to coordinate different metals, and we illustrated this by immobilizing 0.27 at% of iridium (Table 2, entry 7) on **4g** to give **6** (Scheme 2).[46–48] Work is ongoing for the use of **6** in homogeneous supported catalysis.

In conclusion, we have presented a new, straightforward, gram-scale, cheap, and atom-efficient method for the implementation of alkynyl functional groups at the surface of different nanocarbons (namely MWNTs, SWNTs, and graphene). A two-step nucleophilic addition and electrophilic trapping route is involved. We have proven its efficiency with the help of TGA-MS and Raman analysis, either on nanotubes or less reactive exfoliated graphene sheets. We have also shown that this process preserves the electrical properties of CNTs more efficiently than the currently available alternative method. The grafted triple bonds were further utilized with azide-tagged substrates through the well-known click-Huisgen reaction. We have shown the versatility of this method by attaching various molecules for diverse applications.

Acknowledgements

Conflict of Interest

The authors declare no conflict of interest.

[1] A. Hirsch, *Angew. Chem. Int. Ed.* **2002**, *41*, 1853–1859; *Angew. Chem.* **2002**, *114*, 1933–1939.
[2] N. Karousis, N. Tagmatarchis, D. Tasis, *Chem. Rev.* **2010**, *110*, 5366–5397.
[3] D. Tasis, N. Tagmatarchis, A. Bianco, M. Prato, D. Tasis, N. Tagmatarchis, A. Bianco, M. Prato, *Chem. Rev.* **2006**, *106*, 1105–1136.
[4] A. Criado, M. Melchionna, S. Marchesan, M. Prato, *Angew. Chem. Int. Ed.* **2015**, *54*, 10734–10750; *Angew. Chem.* **2015**, *127*, 10882–10900.
[5] F. R. Baptista, S. A. Belhout, S. Giordani, S. J. Quinn, *Chem. Soc. Rev.* **2015**, *44*, 4433–4453.
[6] G. Hong, S. Diao, A. L. Antaris, H. Dai, *Chem. Rev.* **2015**, *115*, 10816–10906.
[7] Z. Spitalsky, D. Tasis, K. Papagelis, C. Galiotis, *Prog. Polym. Sci.* **2010**, *35*, 357–401.
[8] Z. Li, Z. Liu, H. Sun, C. Gao, *Chem. Rev.* **2015**, *115*, 7046–7117.
[9] J. Du, S. Pei, L. Ma, H. M. Cheng, *Adv. Mater.* **2014**, *26*, 1958–1991.
[10] Z. Yang, J. Ren, Z. Zhang, X. Chen, G. Guan, L. Qiu, Y. Zhang, H. Peng, *Chem. Rev.* **2015**, *115*, 5159–5223.
[11] M. R. Axet, O. Dechy-Cabaret, J. Durand, M. Gouygou, P. Serp, *Coord. Chem. Rev.* **2016**, *308*, 236–345.
[12] P. J. Boul, J. Liu, E. T. Mickelson, C. B. Huffman, L. M. Ericson, I. W. Chiang, K. A. Smith, D. T. Colbert, R. H. Hauge, J. L. Margrave, R. E. Smalley, *Chem. Phys. Lett.* **1999**, *310*, 367–372.
[13] R. K. Saini, I. W. Chiang, H. Peng, R. E. Smalley, W. E. Billups, R. H. Hauge, J. L. Margrave, *J. Am. Chem. Soc.* **2003**, *125*, 3617–3621.
[14] O. Roubeau, A. Lucas, A. Pénicaud, A. Derré, *J. Nanosci. Nanotechnol.* **2007**, *7*, 3509–3513.
[15] Y. Maeda, T. Kato, T. Hasegawa, M. Kako, T. Akasaka, J. Lu, S. Nagase, *Org. Lett.* **2010**, *12*, 996–999.
[16] Y. Maeda, K. Saito, N. Akamatsu, Y. Chiba, S. Ohno, Y. Okui, M. Yamada, T. Hasegawa, M. Kako, T. Akasaka, *J. Am. Chem. Soc.* **2012**, *134*, 18101–18108.
[17] Z. Syrgiannis, F. Hauke, J. Röhrl, M. Hundhausen, R. Graupner, Y. Elemes, A. Hirsch, *Eur. J. Org. Chem.* **2008**, 2544–2550.
[18] B. Gebhardt, R. Graupner, F. Hauke, A. Hirsch, *Eur. J. Org. Chem.* **2010**, 1494–1501.
[19] M. K. Bayazit, A. Suri, K. S. Coleman, *Carbon* **2010**, *48*, 3412–3419.
[20] B. Gebhardt, Z. Syrgiannis, C. Backes, R. Graupner, F. Hauke, A. Hirsch, *J. Am. Chem. Soc.* **2011**, *133*, 7985–7995.
[21] L. J. Brennan, Y. K. Gun'ko, *Organometallics* **2015**, *34*, 2086–2097.
[22] R. Huisgen, *Angew. Chem. Int. Ed. Engl.* **1963**, *2*, 565–598; *Angew. Chem.* **1963**, *75*, 604–637.
[23] H. C. Kolb, M. G. Finn, K. B. Sharpless, *Angew. Chem. Int. Ed.* **2001**, *40*, 2004–2021; *Angew. Chem.* **2001**, *113*, 2056–2075.
[24] V. V. Rostovtsev, L. G. Green, V. V. Fokin, K. B. Sharpless, *Angew. Chem. Int. Ed.* **2002**, *41*, 2596–2599; *Angew. Chem.* **2002**, *114*, 2708–2711.
[25] T. Wu, Y. J. Yuan, *Mater. Lett.* **2014**, *133*, 64–66.
[26] X. Su, Y. Shuai, Z. Guo, Y. Feng, *Molecules* **2013**, *18*, 4599–4612.
[27] S. Kantheti, R. R. Gaddam, R. Narayan, K. V. S. N. Raju, *RSC Adv.* **2014**, *4*, 24420–24427.
[28] A. Battigelli, J. T. W. Wang, J. Russier, T. Da Ros, K. Kostarelos, K. T. Al-Jamal, M. Prato, A. Bianco, *Small* **2013**, *9*, 3610–3619.
[29] M. S. Ramasamy, S. S. Mahapatra, J. W. Cho, *J. Colloid Interface Sci.* **2015**, *455*, 63–70.
[30] J. L. Bahr, J. Yang, D. V. Kosynkin, J. Bronikowski, R. E. Smalley, J. M. Tour, M. J. Bronikowski, *J. Am. Chem. Soc.* **2001**, *123*, 6536–6542.
[31] J. L. Bahr, J. M. Tour, *Chem. Mater.* **2001**, *13*, 3823–3824.
[32] S. Campidelli, B. Ballesteros, A. Filoramo, D. D. Díaz, G. De La Torre, T. Torres, G. M. A. Rahman, C. Ehli, D. Kiessling, F. Werner, V. Sgobba, D. M.

Guldi, C. Cioffi, M. Prato, J.-P. Bourgoin, *J. Am. Chem. Soc.* **2008**, *130*, 11503–11509.

[33] G. Tuci, C. Vinattieri, L. Luconi, M. Ceppatelli, S. Cicchi, A. Brandi, J. Filippi, M. Melucci, G. Giambastiani, *Chem. Eur. J.* **2012**, *18*, 8454–8463.

[34] M. Castelaín, P. S. Shuttleworth, C. Marco, G. Ellis, H. J. Salavagione, *Phys. Chem. Chem. Phys.* **2013**, *15*, 16806–16811.

[35] J. Greenwood, T. H. Phan, Y. Fujita, Z. Li, O. Ivasenko, W. Vanderlinden, H. Van Gorp, W. Frederickx, G. Lu, K. Tahara, Y. Tobe, H. Uji-i, S. F. L. Mertens, S. De Feyter, *ACS Nano* **2015**, *9*, 5520–5535.

[36] L. M. Malard, M. A. Pimenta, G. Dresselhaus, M. S. Dresselhaus, *Phys. Rep.* **2009**, *473*, 51–87.

[37] S. Deng, Y. Zhang, A. H. Brozena, M. L. Mayes, P. Banerjee, W.-A. Chiou, G. W. Rubloff, G. C. Schatz, Y. Wang, *Nat. Commun.* **2011**, *2*, 382.

[38] F. M. Smits, *Bell Syst. Tech. J.* **1958**, *37*, 711–718.

[39] K. Sivakumar, F. Xie, B. M. Cash, S. Long, H. N. Barnhill, Q. Wang, *Org. Lett.* **2004**, *6*, 4603–4606.

[40] V. Polshettiwar, R. Luque, A. Fihri, H. Zhu, M. Bouhrara, J. M. Basset, *Chem. Rev.* **2011**, *111*, 3036–3075.

[41] Q. M. Kainz, O. Reiser, *Acc. Chem. Res.* **2014**, *47*, 667–677.

[42] D. Wang, C. Deraedt, L. Salmon, C. Labrugère, L. Etienne, J. Ruiz, D. Astruc, *Chem. Eur. J.* **2015**, *21*, 1508–1519.

[43] R. Soleyman, S. Hirbod, M. Adeli, *Biomater. Sci.* **2015**, *3*, 695–711.

[44] R. Alshehri, A. M. Ilyas, A. Hasan, A. Arnaout, F. Ahmed, A. Memic, *J. Med. Chem.* **2016**, *59*, 8149.

[45] E. Vivès, J. Schmidt, A. Pèlegrin, *Biochim. Biophys. Acta Rev. Cancer* **2008**, *1786*, 126–138.

[46] D. Urankar, B. Pinter, A. Pevec, F. De Proft, I. Turel, J. Kosmrlj, *Inorg. Chem.* **2010**, *49*, 4820–4829.

[47] K. J. Kilpin, E. L. Gavey, C. J. Mcadam, C. B. Anderson, S. J. Lind, C. C. Keep, K. C. Gordon, J. D. Crowley, *Inorg. Chem.* **2011**, *50*, 6334–6346.

[48] M. Valencia, H. Müller-Bunz, R. A. Gossage, M. Albrecht, *Chem. Commun.* **2016**, *52*, 3344–3347.